

Rashba Spin-Orbit Coupling Probed by the Weak Antilocalization Analysis in InAlAs/InGaAs/InAlAs Quantum Wells as a Function of Quantum Well Asymmetry

Takaaki Koga,* Junsaku Nitta, Tatsushi Akazaki, and Hideaki Takayanagi

NTT Basic Research Laboratories, Nippon Telegraph and Telephone Corporation, 3-1 Morinosato-Wakamiya, Atsugi, Kanagawa 243-0198, Japan

(Received 3 October 2001; published 2 July 2002)

We have investigated the values of the Rashba spin-orbit coupling constant α in $\text{In}_{0.52}\text{Al}_{0.48}\text{As}/\text{In}_{0.53}\text{Ga}_{0.47}\text{As}/\text{In}_{0.52}\text{Al}_{0.48}\text{As}$ quantum wells using the weak antilocalization (WAL) analysis as a function of the structural inversion asymmetry (SIA) of the quantum wells. We have found that the deduced α values have a strong correlation with the degree of SIA of the quantum wells as predicted theoretically. The good agreement between the theoretical and experimental values of α suggests that our WAL approach for deducing α values provides a useful tool in designing future spintronics devices that utilize the Rashba spin-orbit coupling.

DOI: 10.1103/PhysRevLett.89.046801

PACS numbers: 72.25.Dc, 72.25.Rb, 73.20.Fz, 73.63.Hs

There has been growing interest in the field of “spintronics” [1], which involves exploration of the extra degrees of freedom provided by electron spin, in addition to those due to electron charge, with a view to realizing new functionalities in future electronic devices. One key to realizing such a spin device is the utilization of the spin-orbit (SO) interaction caused by structural inversion asymmetry (SIA) (Rashba term) in quantum wells (QWs) [2], which can be artificially controlled by controlling the applied gate voltages [3–6] and/or by the specific design of the heterostructure [7]. However, it still remains controversial whether or not the Rashba term really exists in asymmetric QWs from both the theoretical [8–10] and the experimental standpoints [11,12]. From the experimental point of view, the controversy arises from the difficulties in the experimental determination of the Rashba SO coupling constant α . While the existence of a spin splitting Δ at the Fermi energy suggests beating in the Shubnikov–de Haas (SdH) oscillations [3–6], the Δ value deduced from the position of the beating node is usually different from the value of the zero-field spin splitting Δ_0 since Δ includes the effect of the Zeeman spin splitting in a finite magnetic field [13]. In addition, in order for the beating to be observed, the value of Δ has to be sufficiently large so that the SdH oscillation is visible at magnetic fields where the beating nodes are supposed to occur. One should also be careful about the beatinglike patterns in the SdH oscillations that are not really related to Δ . When the position of the Fermi energy is sufficiently close to the second lowest subband edge (within an order of $k_B T$) and significant intersubband scattering is taking place, beatinglike patterns can be observed in the SdH oscillations [14,15]. Also a slight occupation of the second lowest subband itself may produce a beatinglike pattern as well [16]. Therefore, it is essential to develop some other independent experimental techniques for the determination of α values, that are more reliable and reproducible than the SdH beating pattern analysis, in order to clarify the fundamental issues on the Rashba SO coupling. A quantitative understanding of the Rashba

mechanism is also important for realizing future spintronics devices such as the spin field-effect transistor (FET) [17], spin interference devices [18,19], and a nonmagnetic spin filter using a resonant tunneling structure [20].

In this Letter, we propose the use of weak antilocalization (WAL) analysis as a reliable tool to determine Δ_0 values in asymmetric QWs. In fact, the WAL analysis was utilized for studying Δ_0 values by several research groups in the past. Chen *et al.* [7] and Dresselhaus *et al.* [21] have analyzed the low-field magnetoresistance (MR) data for $\text{AlSb}(\text{ZnTe})/\text{InAs}/\text{AlSb}$ and $\text{AlGaAs}/\text{GaAs}/\text{AlGaAs}$ QWs using the WAL theory developed by Hikami, Larkin, and Nagaoka (HLN) [22] and found that the only viable spin-relaxation mechanism is the D’yakonov-Perel’ (DP) mechanism [23] in these systems. Hassenkam *et al.* [24] and Knap *et al.* [25] pointed out, however, that the HLN theory, which assumes the Elliot mechanism [26] for the spin relaxation, does not provide a quantitative fitting to the measured MR data for systems whose spin relaxation is governed by the DP mechanism. It is found that a more quantitative fitting is possible with the model developed by Iordanskii, Lyanda-Geller and Pikus (ILP) [27], in which the effect of Δ_0 is readily included in the theory. Although the WAL analysis using the ILP theory is quite successful in analyzing the measured MR data of asymmetric quantum wells [24,25], there has been no systematic work, to our knowledge, on the quantitative comparison between the experimental values of Δ_0 , which are deduced from the WAL analysis using the ILP model, and the theoretically predicted values of the Rashba spin splitting Δ_R , for a wide range of SIA of the QWs that is controlled by both the specific design of the heterostructures and the applied gate voltage.

Shown in Fig. 1 are the results of self-consistent Poisson-Schrödinger calculations for the four MOCVD-grown samples that were used in this work. These four samples, consisting of an $\text{In}_{0.52}\text{Al}_{0.48}\text{As}/\text{In}_{0.53}\text{Ga}_{0.47}\text{As}/\text{In}_{0.52}\text{Al}_{0.48}\text{As}$ QW, were designed in such a way that only the lowest subband is occupied by the electrons. Recently,

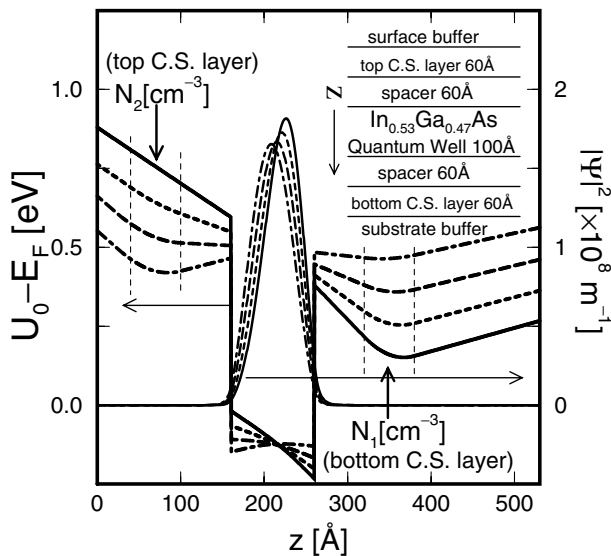


FIG. 1. Calculated potential energies relative to the Fermi energy (left scale) and the squared wave functions (right scale) for the samples used in this paper. The solid, short-dashed, long-dashed, and dash-dotted curves, respectively, denote the results for samples 1–4 defined in Table I. These results were obtained for the carrier density $N_s = 7 \times 10^{11} \text{ cm}^{-2}$. The inset shows the schematic layer structure for these samples, where “C.S. layer” denotes “carrier supplying layer”.

we have found, from the analysis using the HLN theory, that the value of the spin-orbit relaxation time (τ_{SO}) for the QWs of this type is inversely proportional to that of the transport relaxation time (τ_{tr}), suggesting that τ_{SO} is governed by the DP mechanism [16,28]. In addition, the deduced value of Δ_0 from this analysis was consistent with the theoretically predicted value of Δ_R . In this work, we introduce two separate carrier supplying (C.S.) layers in the samples, as shown in the inset of Fig. 1, to control the degree of SIA by the amount of the dopants in these C.S. layers (we denote the impurity densities in the top and bottom C.S. layers by N_2 and N_1 , respectively). While the sum of N_1 and N_2 is kept constant ($4 \times 10^{18} \text{ cm}^{-3}$) in all samples, the ratio between N_1 and N_2 (N_2/N_1) is varied systematically from 0 to 3. It is noted that samples 1 and 4 are designed to be the most and least asymmetric QWs, respectively, for $N_s = 7 \times 10^{11} \text{ cm}^{-2}$, where N_s is the sheet carrier density that can be controlled by the applied gate voltage.

The as-grown samples described above were patterned into $20 \times 80 \mu\text{m}$ Hall bar structures using standard photolithography and lift-off techniques before various electric properties of the confined two-dimensional electron gases (2DEG) were measured as a function of external magnetic

TABLE I. Impurity concentrations used in the present samples.

	Sample 1	Sample 2	Sample 3	Sample 4
$N_1 [\text{cm}^{-3}]$	4×10^{18}	3×10^{18}	2×10^{18}	1×10^{18}
$N_2 [\text{cm}^{-3}]$	0×10^{18}	1×10^{18}	2×10^{18}	3×10^{18}

field B . A SiO_2 layer about 1000 \AA thick was deposited to cover the entire Hall bar mesa to provide a good gate insulation, where the gate electrodes (1500-\AA -thick Au) were deposited on top of the SiO_2 . The values of the carrier mobility at $B = 0 \text{ T}$ for these samples, which were measured at 0.3 K using the standard lock-in technique, were typically $50000 \text{ cm}^2/\text{Vs}$ for $N_s = 1 \times 10^{12} \text{ cm}^{-2}$. All transport measurements were performed in a ^3He cryostat (0.3 K) equipped with a 9 T superconducting magnet, where the magnetic field was applied perpendicular to the heterointerfaces.

Figure 2 shows the measured electric resistances [denoted by $R_{xx}(B)$] as a function of B for samples 1–4, where the fitted curves were provided by the ILP model including only the Rashba (isotropic) term for the spin splitting (see below). In these measurements, the carrier densities N_s for samples 1–4 were adjusted by controlling the applied gate voltages so that they lie between 7.1 and $7.3 \times 10^{11} \text{ cm}^{-2}$, where the corresponding $R_{xx}(0)$ values were found to lie between 1200 and 1600Ω at $B = 0 \text{ T}$. In Fig. 2, we find a pronounced transition from positive to negative MR as we scan the experimental results from sample 1 to sample 4, where the degree of SIA in the QW is systematically varied from a large to a small value, as shown in Fig. 1. This observation indicates that the SO interaction is reduced (τ_{SO} is increased) significantly as the degree of SIA of the QW is decreased. While a similar

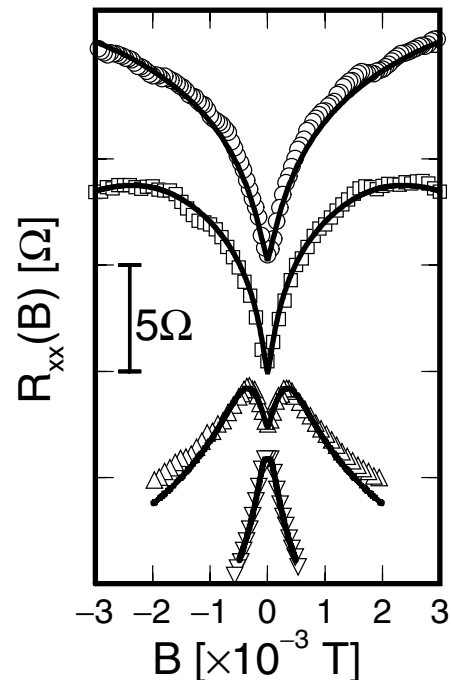


FIG. 2. Low-field magnetoresistance data for samples 1 (○), 2 (□), 3 (△), and 4 (▽). The experiments were performed for sheet carrier densities N_s between 7.1 and $7.3 \times 10^{11} \text{ cm}^{-2}$. The electric resistances at $B = 0 \text{ T}$ ranged from 1200 to 1600Ω depending on the samples in these measurements. The fittings to the experimental data are provided using the model developed by Iordanskii, Lyanda-Geller, and Pikus [27].

transition from a positive to negative MR was observed previously in diffusive Mg films as a function of Au impurity density [29] (where τ_{SO} is controlled by the Elliott mechanism), this is the first observation of the equivalent effect in 2DEGs, to the best of our knowledge, as a function of the SIA of a QW (τ_{SO} is controlled by the DP mechanism).

The fitted curves in Fig. 2 are provided using the model developed by Iordanskii, Lyanda-Geller, and Pikus [27] including only the Rashba term for the spin splitting ($\Omega_3 = 0$ in Refs. [25,27]). Note that Ω_1 in Refs. [25,27] is defined to be half of Δ_0 in this paper ($\Delta_0 = 2\Omega_1$). Since the transport relaxation time τ_{tr} , in the ILP model, gives merely a shift in the conductivity correction $\Delta\sigma(B)$ [25,27], the fitting parameters that fit the experimental data are provided by H_ϕ and H_{SO} only, the magnetic fields relevant to the inelastic and spin-orbit relaxation times, respectively:

$$H_\phi = \frac{\hbar}{4De\tau_\phi}, \quad H_{SO} = \frac{1}{4\hbar De} 2\Omega_1^2 \tau_{tr}. \quad (1)$$

In Eq. (1), D is the diffusion constant for the pertinent 2DEG ($D = v_F^2 \tau_{tr}/2$, where v_F is the Fermi velocity) and τ_ϕ is the inelastic relaxation time. We deduce the values of τ_ϕ and Ω_1 from the fittings of the experimental data, whereas N_s , D , v_F , and τ_{tr} are obtained from the transport (Hall and SdH) measurements using the nonparabolic dispersion relation $\hbar^2 k_{||}^2 / 2m_0^* = E(1 + E/E_g^*)$. Here, $k_{||}$ and E are the in-plane wave number and the energy for an electron in the 2DEG, respectively, m_0^* is the band edge effective mass for the pertinent 2DEG, and E_g^* is the effective band gap energy between the conduction and valence subband edges. While the value of m_0^* ($m_0^* = 0.041m_0$, where m_0 is the free electron mass) was determined from the temperature dependence of the SdH oscillation amplitude, the value of E_g^* ($E_g^* = 0.883$ eV) was chosen to be a little larger than the band gap energy for bulk $\text{In}_{0.53}\text{Ga}_{0.47}\text{As}$ ($E_g = 0.783$ eV) to take into account the quantum confinement effect in our analysis. We were unable to observe the beating patterns in the SdH oscillations with the present samples because the SdH oscillations were visible only above ~ 2 T, whereas the predicted node positions for beating are below 1.5 T even for sample 1. The invisibility of the SdH oscillations below ~ 2 T is not inconsistent with the fact that a single-particle relaxation time τ_s at a finite B could be an order of magnitude smaller than τ_{tr} [30].

Plotted in Fig. 3 are the α values for samples 1–4 deduced as described above using the relation $\Delta_0 = 2\alpha k_F$ (k_F is the Fermi wave number), together with the theoretical values of α obtained from the $\mathbf{k} \cdot \mathbf{p}$ calculations (see below). In the inset of Fig. 3, we also find excellent agreement between the theoretical values of Δ_R and the experimental values of Δ_0 for all the samples investigated. The agreement between Δ_R and Δ_0 suggests that the contribution from the Dresselhaus term to Δ_0 (k^3 term) [31], which arises from crystal inversion asymmetry, is negli-

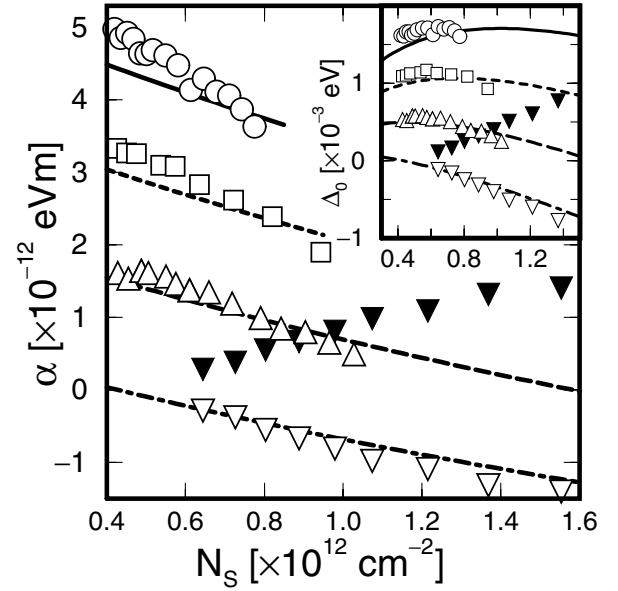


FIG. 3. The α values deduced from the weak antilocalization analysis for samples 1 (○), 2 (□), 3 (△) and 4 (▽ and ▼) together with the theoretical results of the $\mathbf{k} \cdot \mathbf{p}$ calculations (the solid, short-dashed, long-dashed and dash-dotted curves denote the results for samples 1–4, respectively). Our analysis can provide only the absolute values of α . The behavior of α values for sample 4 becomes consistent with the theoretical prediction if we assign negative values to α for this sample (▽). The inset shows the corresponding results in Δ_0 .

ble in the present system. Further investigations are necessary to clarify this issue in more detail.

The theoretical calculation of α values at Fermi energy was performed using the $\mathbf{k} \cdot \mathbf{p}$ formalism, including both the field and boundary contributions to α [4,5]:

$$\alpha = \frac{\hbar^2 E_p}{6m_0} \left\langle \Psi(z) \left| \frac{d}{dz} \left(\frac{1}{E_F - E_{\Gamma_7}(z)} - \frac{1}{E_F - E_{\Gamma_8}(z)} \right) \right| \Psi(z) \right\rangle, \quad (2)$$

where $\Psi(z)$ is the wave function for the confined electrons, E_p is the $\mathbf{k} \cdot \mathbf{p}$ interaction parameter [4,5], E_F is the Fermi energy, and $E_{\Gamma_7}(z)$ and $E_{\Gamma_8}(z)$ are the positions of the band edge energies for Γ_7 (spin split-off band) and Γ_8 (the highest valence band) bands, respectively, at position z . It is noted that the value of E_F was approximated by the conduction band edge energy (E_{Γ_6}) in Refs. [4,5] to simplify the calculation. We have found that this approximation would increase the calculated α values by 20%–30% when the position of E_F is 70–90 meV above the conduction band edge. Therefore, it should be emphasized that our α values are obtained *without* this approximation. We also made a careful treatment of the boundary condition at the substrate-buffer layer interface, where our samples were engineered, using a specific p -type doping at the interface, in such a way that the Fermi energy is pinned at the valence band edge at the substrate-buffer layer interface. This condition allows us to solve the Poisson and Schrödinger

equations self-consistently without specifying the boundary condition at the sample surface, where the position of the Fermi energy is unknown because the surface is covered with the SiO₂ insulating layer. We, thereby, were able to calculate the α values as a function of N_s without using any fitting parameters.

Because our experimental analysis provides only the absolute values of α , we have the freedom of choosing the sign of α for samples 1–4. We find that, in Fig. 3, the values of α monotonically decrease with increasing N_s for samples 1–3, implying that the degree of SIA decreases with increasing N_s . For sample 4, however, we find that the α values increase with increasing N_s if we assign positive values to α as we did for samples 1–3 (see the closed inverted triangles in Fig. 3). However, this behavior of sample 4 is not consistent with that observed for the other samples. This discrepancy is resolved if we assign negative values to α for sample 4 (see the open inverted triangles in Fig. 3), where we find that α values *decrease* (their absolute values increase) with increasing N_s , which is consistent with the theoretical prediction based on the $\mathbf{k} \cdot \mathbf{p}$ model (See the dash-dotted curve in Fig. 3).

In conclusion, the values of the Rashba spin-orbit coupling constant α for MOCVD-grown In_{0.52}Al_{0.48}As/In_{0.53}Ga_{0.47}As/In_{0.52}Al_{0.48}As quantum wells were investigated using weak antilocalization analysis as a function of the structural inversion asymmetry (SIA) of the QW. We have observed a clear transition from positive to negative magnetoresistance near $B = 0$ T by changing the SIA of the QWs. This provides strong evidence that a zero-field spin splitting Δ_0 is induced and controlled by the SIA of the QWs. We have also found a quantitative agreement between theoretical and experimental values of α as a function of both the SIA and/or the sheet carrier density of the QWs. The quantitative understanding of the relation between the α values and the structural properties of the QWs acquired in this study provides the grounds for future spintronics devices that utilize the Rashba spin-orbit coupling effect.

We thank Dr. H. Yokoyama at NTT Advanced Technologies for sample growth and useful discussions, and Dr. S. Pedersen at Chalmers University of Technology for valuable advice on the WAL analysis in this paper. This work was supported by the NEDO International Joint Research Grant Program.

*Electronic address: koga@will.brl.ntt.co.jp

Also with Nanostructure and Material Property, PRESTO, Japan Science and Technology Corporation (JST).

- [1] G. A. Prinz, *Phys. Today* **48**, No. 4, 58 (1995); G. A. Prinz, *Science* **282**, 1660 (1998).
 [2] E. I. Rashba, *Fiz. Tverd. Tela (Leningrad)* **2**, 1224 (1960) [*Sov. Phys. Solid State* **2**, 1109 (1960)]; Y. A. Bychkov and E. I. Rashba, *J. Phys. C* **17**, 6039 (1984).

- [3] J. Nitta, T. Akazaki, H. Takayanagi, and T. Enoki, *Phys. Rev. Lett.* **78**, 1335 (1997).
 [4] G. Engels, J. Lange, Th. Schäpers, and H. Lüth, *Phys. Rev. B* **55**, R1958 (1997).
 [5] Th. Schäpers, G. Engels, J. Lange, Th. Klocke, M. Hollfelder, and H. Lüth, *J. Appl. Phys.* **83**, 4324 (1998).
 [6] D. Grundler, *Phys. Rev. Lett.* **84**, 6074 (2000).
 [7] G. L. Chen, J. Han, T. T. Huang, S. Datta, and D. B. Janes, *Phys. Rev. B* **47**, 4084 (1993).
 [8] F. J. Ohkawa and Y. Uemura, *J. Phys. Soc. Jpn.* **37**, 1325 (1974).
 [9] A. Därr, J. P. Kotthaus, and T. Ando, in *Proceedings of the 13th International Conference on the Physics of Semiconductors*, edited by F. G. Fumi (North-Holland, Amsterdam, 1976), p. 774.
 [10] P. Pfeffer and W. Zawadzki, *Phys. Rev. B* **59**, R5312 (1999).
 [11] A. C. H. Rowe, J. Nehls, R. A. Stradling, and R. S. Ferguson, *Phys. Rev. B* **63**, 201307(R) (2001).
 [12] S. Brosig, K. Ensslin, R. J. Warburton, C. Nguyen, B. Brar, M. Thomas, and H. Kroemer, *Phys. Rev. B* **60**, 13 989 (1999).
 [13] G. Lommer, F. Malcher, and U. Rössler, *Phys. Rev. Lett.* **60**, 728 (1988).
 [14] T. H. Sander, S. N. Holmes, J. J. Harris, D. K. Maude, and J. C. Portal, *Phys. Rev. B* **58**, 13 856 (1998).
 [15] D. R. Leadley, R. Fletcher, R. J. Nicholas, F. Tao, C. T. Foxon, and J. J. Harris, *Phys. Rev. B* **46**, 12 439 (1992).
 [16] T. Koga, J. Nitta, T. Akazaki, and H. Takayanagi, in *Proceedings of NGS 10*, IPAP Conf. Series Vol. 2 (IPAP, Tokyo, 2001), p. 227.
 [17] S. Datta and B. Das, *Appl. Phys. Lett.* **56**, 665 (1990).
 [18] J. Nitta, F. E. Meijer, and H. Takayanagi, *Appl. Phys. Lett.* **75**, 695 (1999).
 [19] T.-Z. Qian and Z.-B. Su, *Phys. Rev. Lett.* **72**, 2311 (1994).
 [20] T. Koga, J. Nitta, H. Takayanagi, and S. Datta, *Phys. Rev. Lett.* **88**, 126601 (2002).
 [21] P. D. Dresselhaus, C. M. A. Papavassiliou, R. G. Wheeler, and R. N. Sacks, *Phys. Rev. Lett.* **68**, 106 (1992).
 [22] S. Hikami, A. I. Larkin, and Y. Nagaoka, *Prog. Theor. Phys.* **63**, 707 (1980).
 [23] M. I. D'yakanov and V. I. Perel', *Zh. Eksp. Teor. Fiz.* **60**, 1954 (1971) [*Sov. Phys. JETP* **33**, 1053 (1971)].
 [24] T. Hassenkam, S. Pedersen, K. Baklanov, A. Kristensen, C. B. Sorensen, P. E. Lindelof, F. G. Pikus, and G. E. Pikus, *Phys. Rev. B* **55**, 9298 (1997).
 [25] W. Knap, C. Skierbiszewski, A. Zduniak, E. Litwin-Staszewska, D. Bertho, F. Kobbi, J. L. Robert, G. E. Pikus, F. G. Pikus, S. V. Iordanskii, V. Mosser, K. Zekentes, and Yu. B. Lyanda-Geller, *Phys. Rev. B* **53**, 3912 (1996).
 [26] R. J. Elliott, *Phys. Rev.* **96**, 266 (1954).
 [27] S. V. Iordanskii, Yu. B. Lyanda-Geller, and G. E. Pikus, *JETP Lett.* **60**, 206 (1994).
 [28] T. Koga, J. Nitta, T. Akazaki, and H. Takayanagi, *Physica (Amsterdam)* **13E**, 542 (2002).
 [29] G. Bergmann, *Phys. Rep.* **107**, 1 (1984).
 [30] S. Das Sarma and F. Stern, *Phys. Rev. B* **32**, 8442 (1985).
 [31] G. Dresselhaus, *Phys. Rev.* **100**, 580 (1955).